JOC Article
pubs.acs.org/joc

Mechanism of the Ni(0)-Catalyzed Vinylcyclopropane−Cyclopentene Rearrangement

Selina C. Wang,[†] Dawn M. Troast,[‡] Martin Conda-Sheridan,[‡] Gang Zuo,[‡] Donna LaGarde,[‡] Janis Louie,*[,‡] and Dean J. Tantillo*[,†]

[†]*Department of Chemistry, University of California, Davis, One Shields Avenue, Davis, California 95616, and* [‡]*Department of Chemistry, University of Utah, 315 South 1400 East, Salt Lake City, Utah 84112*

louie@chem.utah.edu; tantillo@chem.ucdavis.edu

Received July 21, 2009

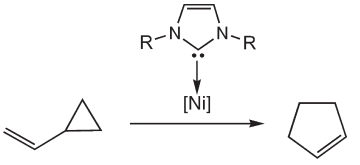

A combination of physical organic experiments and quantum chemical calculations were used to construct a detailed mechanistic model for the Ni(0)-*N*-heterocyclic carbene-catalyzed vinylcyclopropane−cyclopentene rearrangement that involves a mutistep oxidative addition/haptotropic shift/reductive elimination pathway. No evidence for the intermediacy of radicals or zwitterions was found. The roles of substituents on the vinylcyclopropane substrate and variations in the ligands on Ni were evaluated. It is postulated that bulky carbene ligands facilitate formation of the active catalyst species.

Introduction

Whereas transition-metal-promoted cycloadditions have shown tremendous synthetic promise,[1] transition-metal-promoted sigmatropic shifts have not been exploited nearly as frequently.[2−4] However, one sigmatropic shift that has been shown to be amenable to manipulation by transition metals is the [1,3] sigmatropic rearrangement of vinylcyclopropanes to cyclopentenes.[3,4] In the absence of transition metals, Lewis acids, or activating substituents, vinylcyclopropane−cyclopentene rearrangements require high temperatures and tend to produce various byproducts, most of which are thought to arise from alkyl/allyl diradical intermediates (Scheme 1).[5] Various transition metals (e.g., Pd(0),[6] Rh(I),[7] and Ni(0)[8]) have been shown to facilitate vinylcyclopropane−cyclopentene rearrangements, but in many cases, activating groups on the vinylcyclopropane appear to be required (see Scheme 2 for representative examples).

SCHEME 1

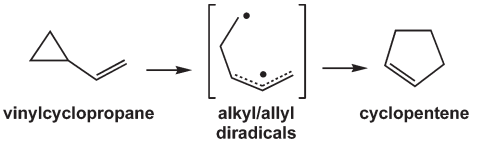

(1) For leading references, see: (a) Lautens, M.; Klute, W.; Tam, W. *Chem. Rev.* **1996**, *96*, 49–92. (b) Fruhauf, H.-W. *Chem. Rev.* **1997**, *97*, 523–596.

(2) (a) Siebert, M. R.; Tantillo, D. J. *J. Am. Chem. Soc.* **2007**, *129*, 8686–8687. (b) Overman, L. E.; Renaldo, A. F. *J. Am. Chem. Soc.* **1990**, *112*, 3945–3949.

(3) Hudlicky, T.; Kutchan, T. M.; Naqvi, S. M. In *Organic Reactions*; Kende, A. S., Ed.; Wiley: New York, 1985; Coll. Vol. 33, Chapter 2.

(4) For a mini-review on metal-promoted vinylcyclopropane−cyclopentene rearrangements, see: Wang, S. C.; Tantillo, D. J. *J. Organomet. Chem.* **2006**, *691*, 4386–4392.

(5) Baldwin, J. E. *Chem. Rev.* **2003**, 1197–1212.

(6) (a) Morizawa, Y.; Oshima, K.; Nozaki, H. *Tetrahedron Lett.* **1982**, *23*, 2871–2874. (b) Fugami, K.; Morizawa, Y.; Oshima, K.; Nozaki, H. *Tetraheron Lett* **1985**, *26*, 857–860. (c) Burgess, K. *J. Org. Chem.* **1987**, *52*, 2046–2051. (d) Burgess, K. *Tetrahedron Lett.* **1985**, *26*, 3049–3052.

(7) (a) Grigg, R.; Hayes, R.; Sweeney, A. *J. Chem. Soc., Chem. Commun.* **1971**, 1248–1249. (b) Alcock, N. W.; Brown, J. M.; Conneely, J. A.; Williamsom, D. H. *J. Chem. Soc., Chem. Commun.* **1975**, 792–793. (c) Aris, V.; Brown, J. M.; Conneely, J. A.; Golding, B. R.; Williamson, D. H. *J. Chem. Soc., Perkin Trans. 2* **1975**, 4–10. (d) Salomon, R. G.; Salomon, M. F.; Kachinski, J. L. C. *J. Am. Chem. Soc.* **1977**, *99*, 1043. (e) Alcock, N. W.; Brown, J. M.; Conneely, J. A.; Williamsom, D. H. *J. Chem. Soc., Perkin Trans. 2* **1979**, 962–971. (f) Hudlicky, T.; Koszyk, F. J.; Kutchan, T. M.; Sheth, J. P *J. Org. Chem.* **1980**, *45*, 5020–5027. (g) Hayashi, M.; Ohmatsu, T.; Meng, Y.-P.; Saigo, K. *Angew. Chem., Int. Ed.* **1998**, *37*, 837–839. (h) Jun, C.-H.; Kang, J.-B.; Lim, Y.-G. *Tetrahedron Lett.* **1995**, *36*, 277–280.

(8) (a) Murakami, M.; Nishida, S. *Chem. Lett.* **1979**, 927–930. (b) Ryu, I.; Ikura, K.; Tamura, Y.; Maenaka, J.; Ogawa, A.; Sonoda, N. *Synlett* **1994**, 941–942. (c) Zuo, G.; Louie, J. *Angew. Chem., Int. Ed.* **2004**, 2227–2229.

Published on Web 09/25/2009 DOI: 10.1021/jo901525u

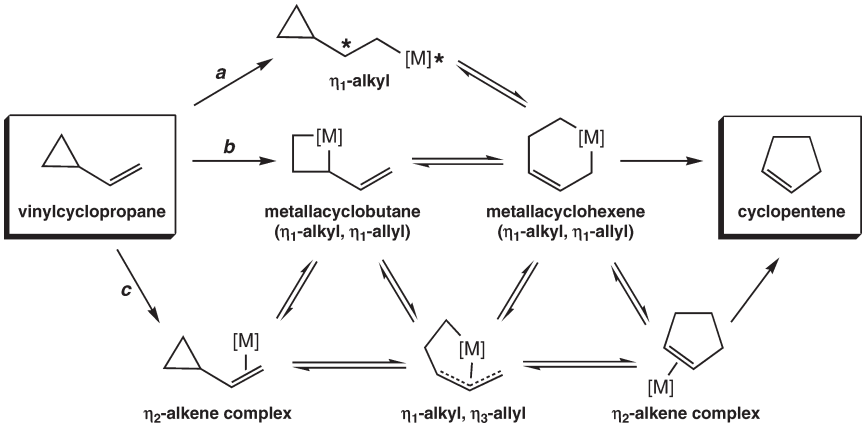

FIGURE 1. Possible mechanistic pathways for the isomerization of vinylcyclopropane to cyclopentene.

SCHEME 2

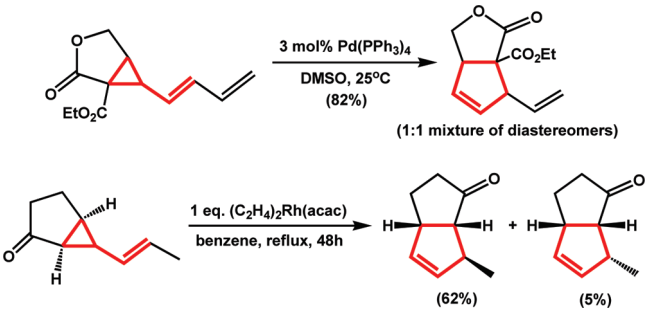

Recently, Louie and co-workers reported that Ni(0)-*N*-heterocyclic carbene (NHC) complexes are effective catalysts for vinylcyclopropane−cyclopentene rearrangements involving unactivated vinylcyclopropane reactants (Table 1).[8c] 1,1-Disubstituted substrates underwent facile rearrangement at room temperature without the aid of activating groups (entry 1). Trisubstituted substrates required slightly elevated temperature (60 °C) (entry 2). 1,2-Disubstituted substrates required both elevated temperature and activation with an aromatic group (entries 3 and 4).

The most likely mechanistic pathways for the metal-promoted isomerization of vinylcyclopropanes are shown in Figure 1.[4] Both radical and zwitterionic mechanisms would form an η_1-alkyl species through initial addition of the metal to the alkene (pathway *a*). Alternatively, oxidative addition to the cyclopropane would lead to a metallacyclobutane intermediate, which could occur with or without initial complexation of the substrate to the metal (pathways *b* and *c*). Which of these pathways occurs for a given experimental system depends on the specific metal and ligands used.[4]

Herein, we describe quantum chemical calculations and physical organic experiments on the mechanism of the Ni(0)-promoted vinylcyclopropane−cyclopentene rearrangement. In addition to proposing a detailed mechanism based on these studies, we also predict the outcome of reactions with a variety of reactants and explore the potential of various non-NHC ligands. The transition state structures we describe in this report should provide important points of departure for the rational design of catalysts for asymmetric versions of this metal-promoted sigmatropic shift.

TABLE 1. Nickel-Catalyzed Isomerization[a] of Various Vinyl Cyclopropanes[8c]

entry	Substrate	Product	T	t [h]	yield [%][b]
1	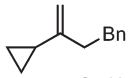	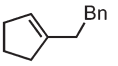	RT	12	93
2	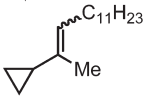	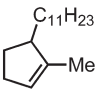	60°C	12	94
3	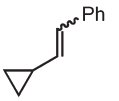		60°C	12	92
4	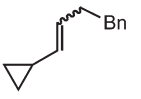	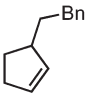	100°C	12	N.R.

[a]Performed with 1.0 mol % [Ni(COD)$_2$], 2.0 mol % IPr, and 0.10 M substrate in toluene, benzene, or hexanes. [b]Yields of isolated products (average of at least two runs). N.R. = no reaction.

Results and Discussion

1. Parent System: Unsubstituted Vinylcyclopropane. Computed Overall Mechanism. We began our theoretical studies (see Computational Methods for details) by computing structures involved in the rearrangement of unsubstituted vinylcyclopropane in the presence of Ni(*N*,*N*′-dimethylimidazolylidene). All of the calculations described herein are based on the assumption that the active catalyst is a Ni(0) species. The computed intermediates (**INT**) and transition state structures (**TS**‡) for this rearrangement are shown in Figure 2, their relative energies are shown in Figure 3, and a summary of the overall computed mechanism is shown in Scheme 3 (note that we do not intend to imply that a free Ni(*N*,*N*′-dimethylimidazolylidene) is generated in solution).

The computed mechanism first involves rearrangement of an initially formed η_2-vinylcyclopropane complex (**INT1**; note that we also located another conformer of **INT1** where the vinylcyclopropane is not oriented appropriately for

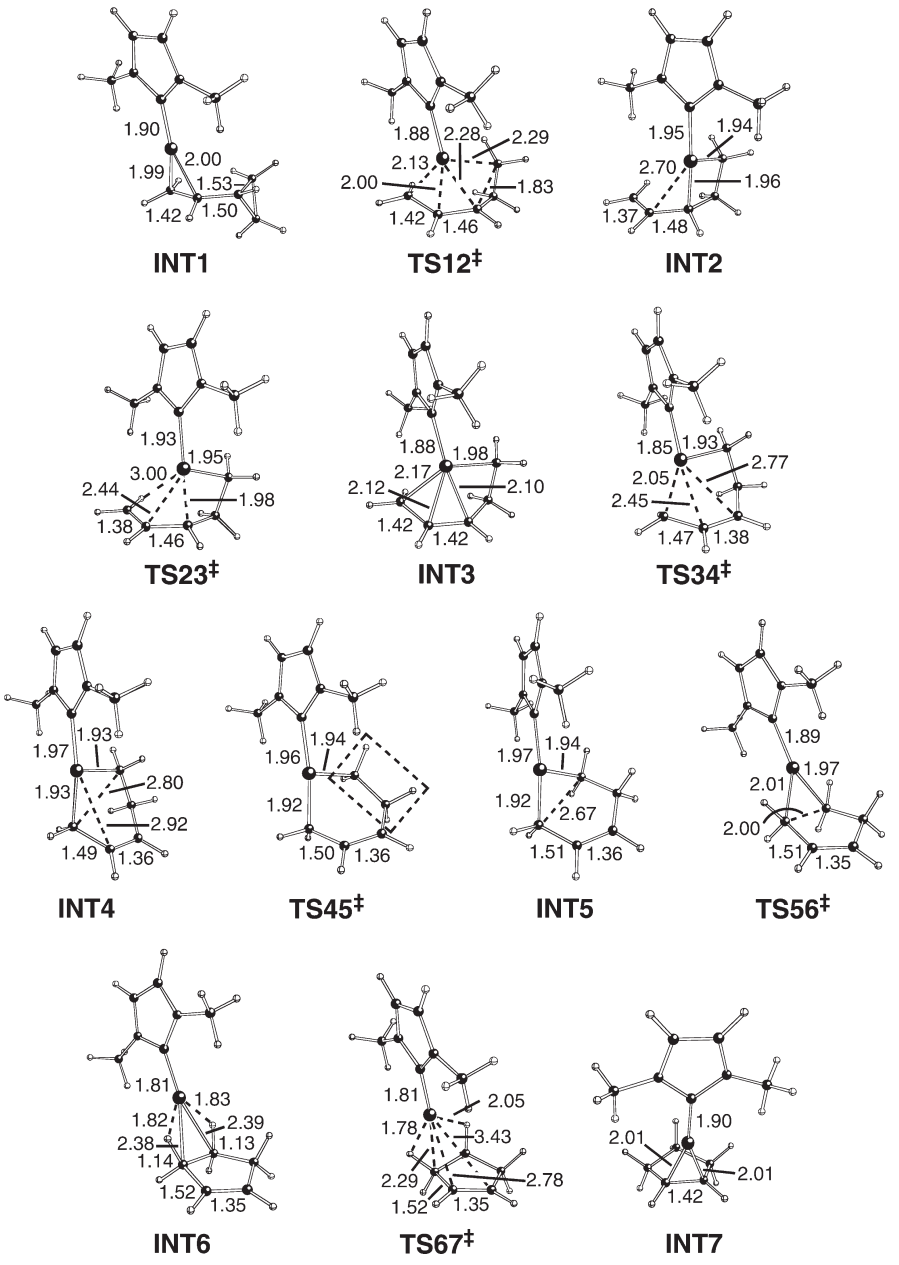

FIGURE 2. Geometries (B3LYP/LANL2DZ; distances in Å; see Computational Methods for details) of intermediates and transition state structures in the Ni(*N*,*N*′-dimethylimidazolylidene)-catalyzed rearrangement of vinylcyclopropane to cyclopentene.

oxidative addition; the energy of this conformer is marked with an **INT1$_b$** label throughout the paper)[9] via oxidative addition to form a vinylmetallacyclobutane (**INT2**). This complex then rearranges to a metallacyclohexene (**INT4**) by way of an η_1-alkyl/η_3-allyl intermediate (**INT3**). **INT4** then undergoes a conformational change (to **INT5**) that prepares it for reductive elimination to form a σ-complex of cyclopentene (**INT6**). This intermediate then rearranges with a very small barrier to a π-complex of cyclopentene (**INT7**).

Several of the intermediates and transition state structures involved in this process have interesting features. First, it is somewhat unusual that the vinylmetallacyclobutane, η_1-alkyl/η_3-allyl, and metallacyclohexene structures are all found as minima. Even though the barrier for conversion of the vinylmetallacyclobutane (**INT2**) to the η_1-alkyl/η_3-allyl (**INT3**) is small enough to be of little chemical consequence (in other words, this portion of the energy surface is rather flat), the barrier for conversion of **INT3** to **INT4** is substantial (greater than 10 kcal/mol; see Figure 3). Note that the Ni−C_{NHC} distance in **TS34**‡ (1.85 Å) is shorter than the corresponding distance in all of the other structures (except the weakly bound σ-complex (**INT6**) and the transition structure (**TS67**‡) for its conversion to **INT7**), hinting that Ni−allyl bonding in this structure is weaker

(9) Geometries of **INT1$_b$** complexes are available in the Supporting Information. For the unsubstituted vinylcyclopropane system, **INT1$_b$** is 1.2 kcal/mol lower in energy than **INT1** (B3LYP/DZVP2+//B3LYP/LANL2DZ + ZPE(B3LYP/LANL2DZ)).

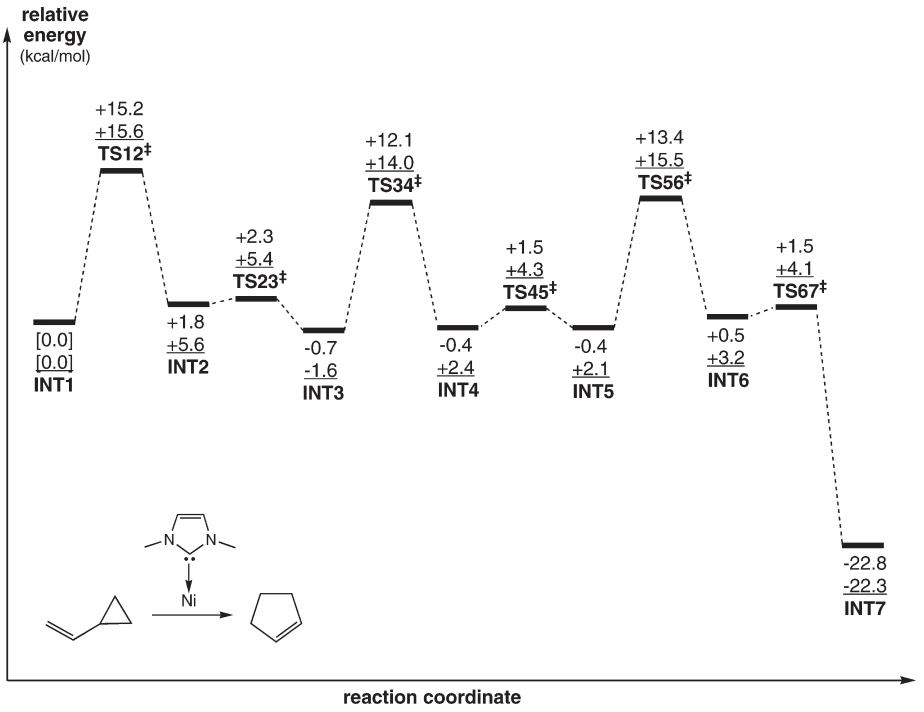

FIGURE 3. Relative energies (B3LYP/LANL2DZ, kcal/mol in normal text; B3LYP/DZVP2+//B3LYP/LANL2DZ + ZPE(B3LYP/LANL2DZ) in underlined text; see Computational Methods for details) of structures shown in Figure 1.

SCHEME 3

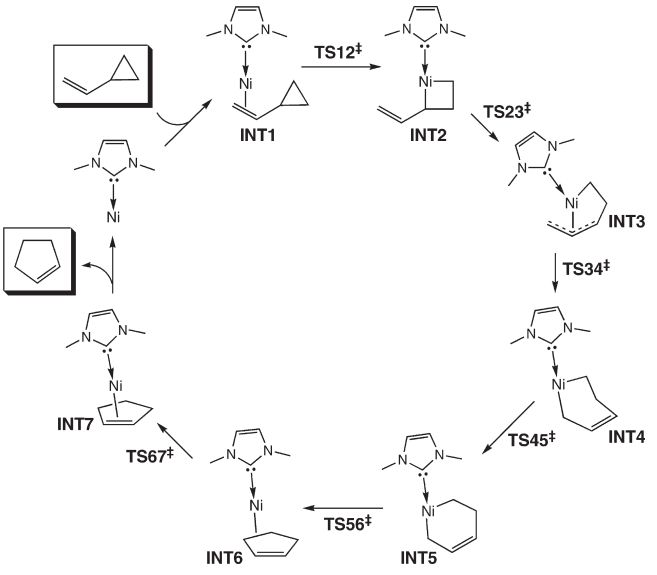

than in the other allyl complexes **INT2**−**INT5**. Second, a crankshaft rotation of the ethylene group in metallacyclohexene **INT4** (dashed box in Figure 2) is necessary to bring the two methylenes attached directly to Ni closer together so that reductive elimination can occur readily. Third, formation of the σ-complex (**INT6**) is also noteworthy. Note that both of the C−H bonds near to the Ni are elongated.

(10) Since the internal and terminal monoalkyl systems are isomers of each other, all of the energies are on the same scale, relative to the energy of the internal substituted h2-vinylcyclopropane **INT1** complex.

While our calculations suggest that the formation of vinylmetallacyclobutane **INT2** is the rate-determining step, energies of the transition state structures for formation of metallacyclohexene **INT4** (**TS34**‡) and σ-complex **INT6** (**TS56**‡) are only very slightly lower in energy, respectively. All of the intermediates that we located (**INT1**−**INT6**) have similar energies (spanning only a few kcal/mol), while the product π-complex **INT7** is much lower in energy, reflecting the energy difference between σ- and π-complexation of cyclopentene; interestingly, throughout the reaction there appears to be a balance of strain and Ni−carbon bonding.

Likelihood of Diradical or Zwitterionic Intermediates. Several additional mechanistic possibilities were also explored. First, we considered the possibility that diradical species might be involved (e.g., Figure 1, path a). Using a system with a 2-methyl group (for additional details on this particular system, see below), the triplet diradical counterpart of **INT1** was located as a minimum (using UB3LYP/LANL2DZ), and this structure is ~23 kcal/mol higher in energy than **INT1**. Similarly, the triplet diradical analogue of **INT4** was 6 kcal/mol higher in energy than **INT4** (see Supporting Information for details). On the basis of these results, we did not pursue further calculations on diradicals.

Second, we explored the possibility of zwitterionic intermediates. Here we assessed the energies of species such as **A** (below) by performing constrained optimizations with the indicated bond angle fixed to a value of 109.5°. The energies of the resulting structures (for substrates with alkyl substituents in various positions; see Supporting Information for further details) were generally 15−20 kcal/mol above that of the corresponding **INT1** complexes, i.e., they were generally similar in energy to **TS12**‡. Thus, we think that mechanisms involving such intermediates are unlikely (note that although these are gas phase calculations, the

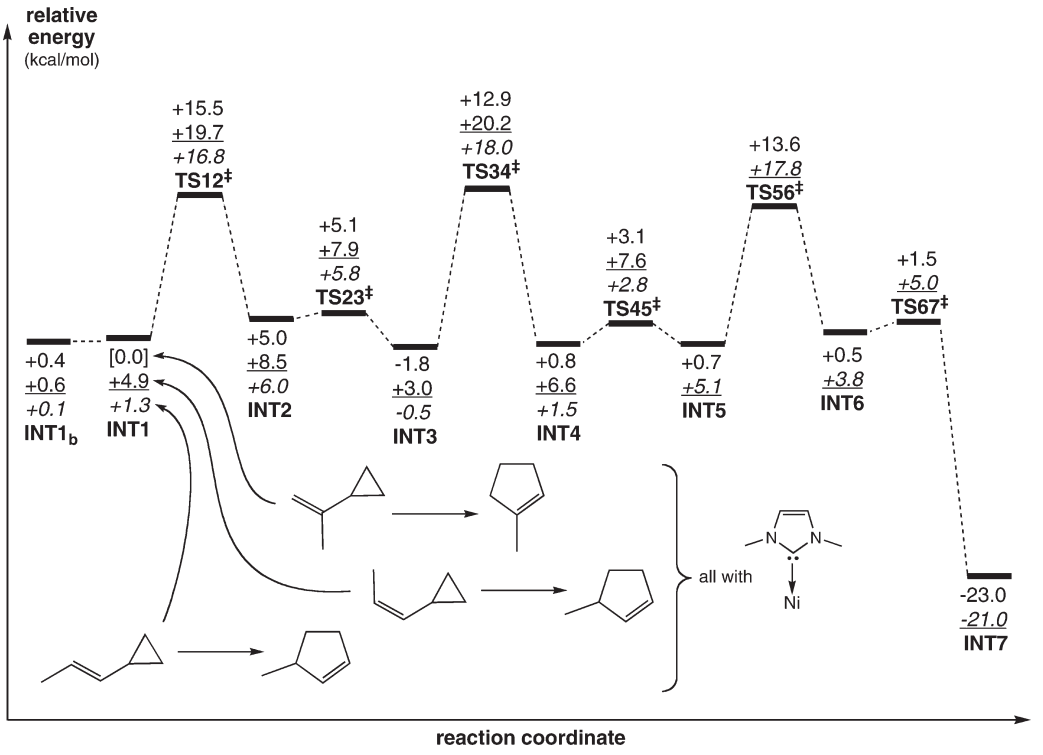

FIGURE 4. Relative energies (B3LYP/DZVP2+//B3LYP/LANL2DZ + ZPE(B3LYP/LANL2DZ), kcal/mol; see Computational Methods for details) of analogues of structures shown in Figure 1 with monomethyl-substituted vinylcyclopropanes.[10]

experimental reactions were carried out in nonpolar aromatic and aliphatic solvents).[8c]

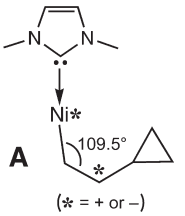

2. Alkyl-Substituted Systems. Monoalkylvinylcyclopropanes. We also examined the effects of alkyl substitution on the rearrangement. As shown in Figure 4, the overall mechanism does not change upon alkyl substitution, although which of the three highest transition state structures is the absolute highest does vary. Interestingly, the reaction coordinates for the *cis*- and *trans*-methylvinylcyclopropane systems actually intersect at **INT5**, and both systems undergo reductive elimination through the same **TS56**‡ (actually, the two paths involve enantiomeric versions of **INT5** and **TS56**‡). This is a result of a conformational change for the *trans* system that allows the Ni to avoid being in close proximity to the methyl group in the last few intermediates and transition state structures.

The experimental results of Zuo and Louie indicate that systems with internal alkyl groups rearrange readily, whereas systems with terminal alkyl groups do not (Table 1; compare entries 1 and 4).[8c] Our calculations are consistent with these observations. The overall barrier for rearrangement of the vinylcyclopropane with an internal methyl group is predicted to be 15.5 kcal/mol, while the barriers for the systems with a terminal methyl group are higher (19.6 and 17.9 kcal/mol, from the lower energy **INT1b** in these cases[9]). Note also that the absolute energies of the transition state structures are lower for the internally substituted system. Moreover, this difference in reactivity is likely to be underestimated in our calculations, given that a small NHC was used in the modeling; given the geometries of the transition structures involved (e.g., Figure 1), we expect steric repulsions to be greater for 1-substitution. The internally substituted system also leads to a trisubstituted alkene, rather than a disubstituted alkene, providing a greater driving force for rearrangement of the internally substituted systems. An internal methyl group is also predicted to accelerate the rearrangement as compared to the unsubstituted system (vide supra), whose overall barrier (from **INT1b**) is computed to be 16.8 kcal/mol.

Dialkylvinylcyclopropanes. Disubstituted vinylcyclopropanes are predicted to behave much like the monosubstituted systems described above (Figure 5). One key difference, however, is observed for the *gem*-dimethyl case. Unlike the *trans* monomethyl case described above, no simple change in conformation can lead to a reductive elimination transition structure where the Ni is not near to a methyl group, and a high energy reductive elimination transition structure is therefore observed (Figure 6, left); again, this steric problem is likely to greater in the experimental system, which involves a bulky NHC. Note also that **TS67**‡ for this system involves migration of the Ni "the long way around" the five-membered ring in order to avoid the methyl group (Figure 6, right).

Although experimental results on *gem*-dialkyl substrates have not been reported (we would predict that the problematic reductive elimination described above in such systems would hinder rearrangements on the basis of our computations), rearrangements of vicinal dialkyl systems

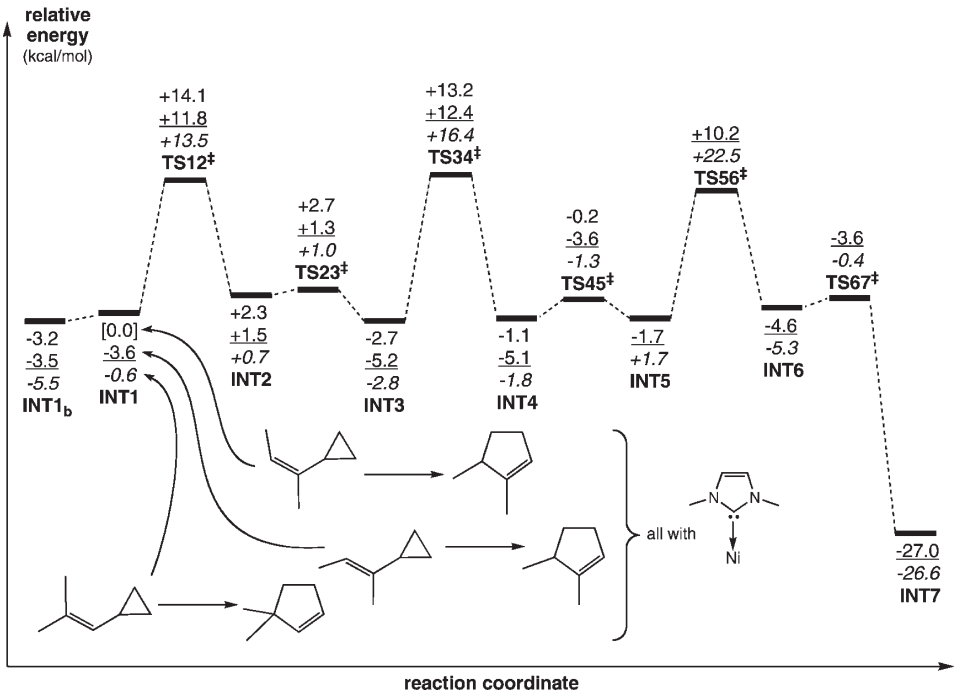

FIGURE 5. Relative energies (B3LYP/DZVP2+//B3LYP/LANL2DZ + ZPE(B3LYP/LANL2DZ), kcal/mol; see Computational Methods section for details) of analogues of structures shown in Figure 1 with dimethyl-substituted vinylcyclopropanes (note that, again, the *cis* and *trans* pathways converge).[10]

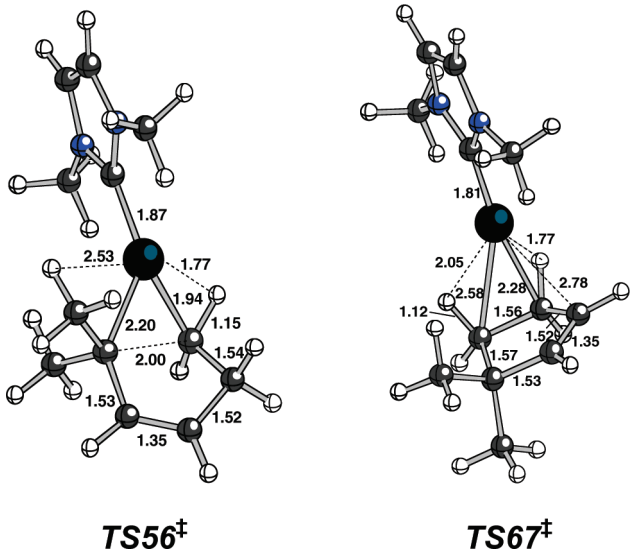

FIGURE 6. Computed geometries (B3LYP/LANL2DZ, distances in Å; see Computational Methods for details) of unusual transition structures from Figure 5.

have been reported.[8c] These systems are observed to rearrange more sluggishly than do monoalkyl-substituted systems with internal alkyl groups, but more readily than do monoalkyl-substituted systems with terminal alkyl groups. Our predicted barriers for the vicinal dimethyl systems (Figure 5) are 17.3 (here, **TS12**‡ is the highest energy structure) and 16.0 kcal/mol (here, **TS34**‡ is the highest energy structure), respectively; interestingly, these barriers are between those computed for systems with internal and terminal methyl groups (vide supra).

Trialkylvinylcyclopropanes. The trimethyl-substituted vinylcyclopropane shown in Figure 7 behaves very much like the *gem*-dimethyl-substituted system described above. Again, we predict that this sort of system will not rearrange efficiently; however, we do predict that the internal alkyl group will lower the overall barrier compared to that for the *gem*-dimethyl-substituted system (23.9 vs 28.0 kcal/mol).

3. Aryl-Substituted Systems. Louie and co-workers showed that phenyl-substituted vinylcyclopropanes rearrange more easily than do related alkyl-substituted cases, for both internal and terminal substituted cases (Tables 1 and 2).[8c] Our calculations do not predict a significant increase in reactivity for the phenyl-substituted systems, however (compare Figure 8 with Figure 4). This discrepancy between experiment and theory perhaps suggests that the main difference between aryl and alkyl substituents in these reactions, in terms of their effects on the overall rearrangement barriers, is predominantly steric rather than electronic in nature, since our calculations capture electronic effects but underestimate steric effects due to the size of our model ligand.

In the case of the *cis*-phenyl-substituted vinylcyclopropane (Figure 8b), we observed a shorter version of our proposed mechanism (Scheme 3). We were unable to locate the vinylmetallacyclobutane complex (**INT2**) and instead found a transition state structure (**TS13**‡, Figure 9a) that connects the η_2-vinylcyclopropane (**INT1**) and η_1-alkyl/η_3-allyl intermediate (**INT3**). Thus, in this case, the very shallow minimum associated with **INT2** disappears. Additionally, it appears that no conformational changes are required before formation of the σ-complex **INT6**.

For the *trans*-phenyl-substituted vinylcyclopropane (Figure 8c), an additional interesting transition state structure was also located (**TS57**$_b$‡, Figure 9b, left). This

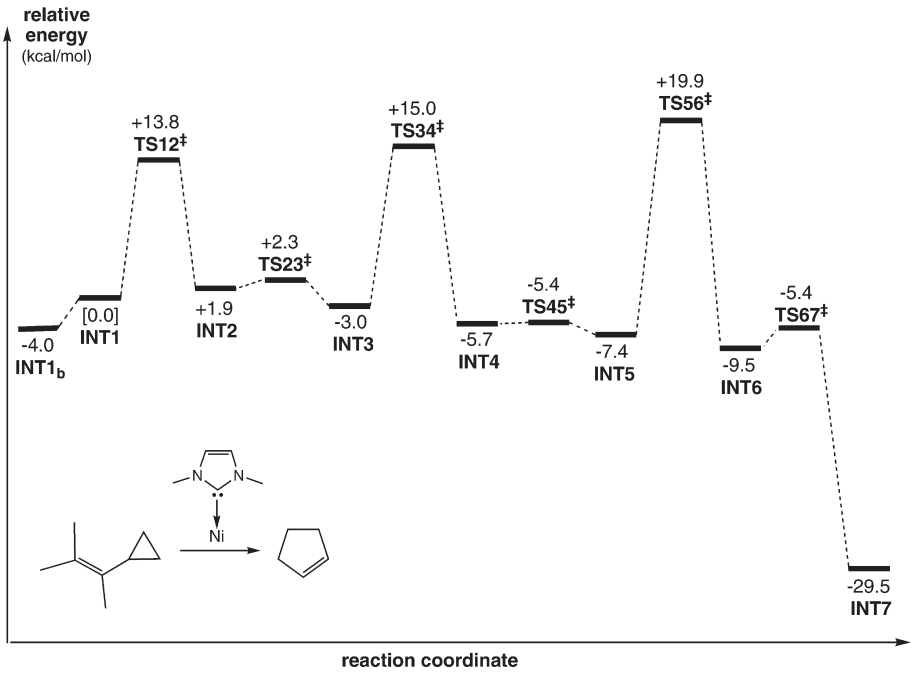

FIGURE 7. Relative energies (B3LYP/DZVP2+//B3LYP/LANL2DZ + ZPE(B3LYP/LANL2DZ), kcal/mol; see Computational Methods for details) of analogues of structures shown in Figure 1 with trisubstituted vinylcyclopropanes.

transition structure leads to a product complex in which the nickel interacts with the π-system of the phenyl group (**INT7$_b$**, Figure 9b, right), rather than the σ-framework of the cyclopentene (**INT6**). **TS57$_b$**‡ is more than 1 kcal/mol higher in energy than **TS46**‡, however.

The reactivity of several phenyl-substituted vinylcyclopropanes was investigated experimentally by determining their rearrangement rates (Table 2). The isomerization of (1-cyclopropylvinyl)benzene (**1**) was significantly faster than that of (*E*)-(2-cyclopropylvinyl)benzene (**2**); note that the rate for **2** (entry 2) was determined at 60 °C, whereas the rate for **1** (entry 1) was determined at 27 °C because the rate of rearrangement for **1** was too fast to measure at 60 °C. This reactivity difference was borne out in our calculations as well (Figure 8). (*Z*)-(1-Cyclopropylprop-1,2-yl)benzene (**3**) isomerizes to the (*E*)-substrate (**2**) before rearrangement (entry 3), so a rearrangement rate was not determined for this specific substrate. When (*E*)-(1-cyclopropylprop-1,2-yl)-benzene (**4**) was subjected to the isomerization conditions, no reaction was observed, even at higher temperatures (60 °C, entry 4). These results are consistent with the unwillingness of *gem*-disubstituted vinylcyclopropanes to rearrange (vide supra).

The initial *cis*−*trans* isomerization of **3** could be explained by a diradical mechanism, but our calculations (vide supra) suggest that this is unlikely. In an attempt to settle this issue, the reaction of **3** was carried out in the presence of TEMPO and BHT (2,6-di-*tert*-butyl-*p*-cresol) in an effort to trap any radical intermediates. Under these conditions, no decrease in conversion or yield was observed, consistent with the absence of radical intermediates.

Substituent Effects. The effect of substituents on the phenyl ring on the rate of rearrangement was also examined (Table 3). Substrates bearing electron-withdrawing groups (entries 1 and 2) were found to rearrange more quickly than the unsubstituted substrate (entry 4), and substrates bearing electron-donating groups (entries 5 and 6) rearranged more slowly. The Hammett plot (Figure 10)[11,12] constructed from this data had a ρ value of 0.11. A ρ value greater than 0.2 is typically considered to indicate a significant substituent effect.[11] Therefore, although substituents on the aryl ring have an effect on the rate of the reaction, this effect is small, consistent with zwitterionic (or radical) mechanisms not contributing significantly. The effect of varying the electron density of the aromatic group was also explored by theoretical calculations, and as shown in Table 3 (last column), the experimentally determined order of reactivity is reflected in the computed rearrangement barriers for processes not involving zwitterionic or diradical intermediates.

4. Other Ligands on Ni. The effect of the structure of the carbene ligand on the rearrangement was also examined by measuring the first-order rate constants for rearrangement with a variety of ligands (Table 4). The rearrangement of (*E*)-(2-cyclopropylvinyl)benzene (**2**) in the presence of 1,3-bis(2,6-diisopropylphenyl)-4,5-dihydroimidazol-2-ylidene

(11) For leading references, see: Hansch, C.; Leo, A.; Taft, R. W. *Chem. Rev.* **1991**, *91*, 165–195.

(12) The activation energy for (*E*)-1-(2-cyclopropylvinyl)-4-fluorobenzene was determined by measuring the first-order rate constant at various temperatures (see below). Application of the Eyring equation led to an activation energy of 27 kcal/mol, which is consistent with the need for elevated temperatures to promote rearrangements of 1,2-disubstituted substrates.

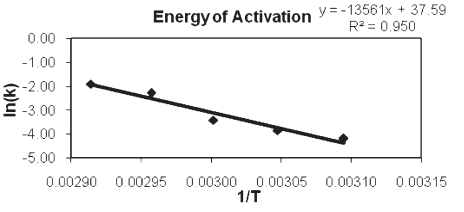

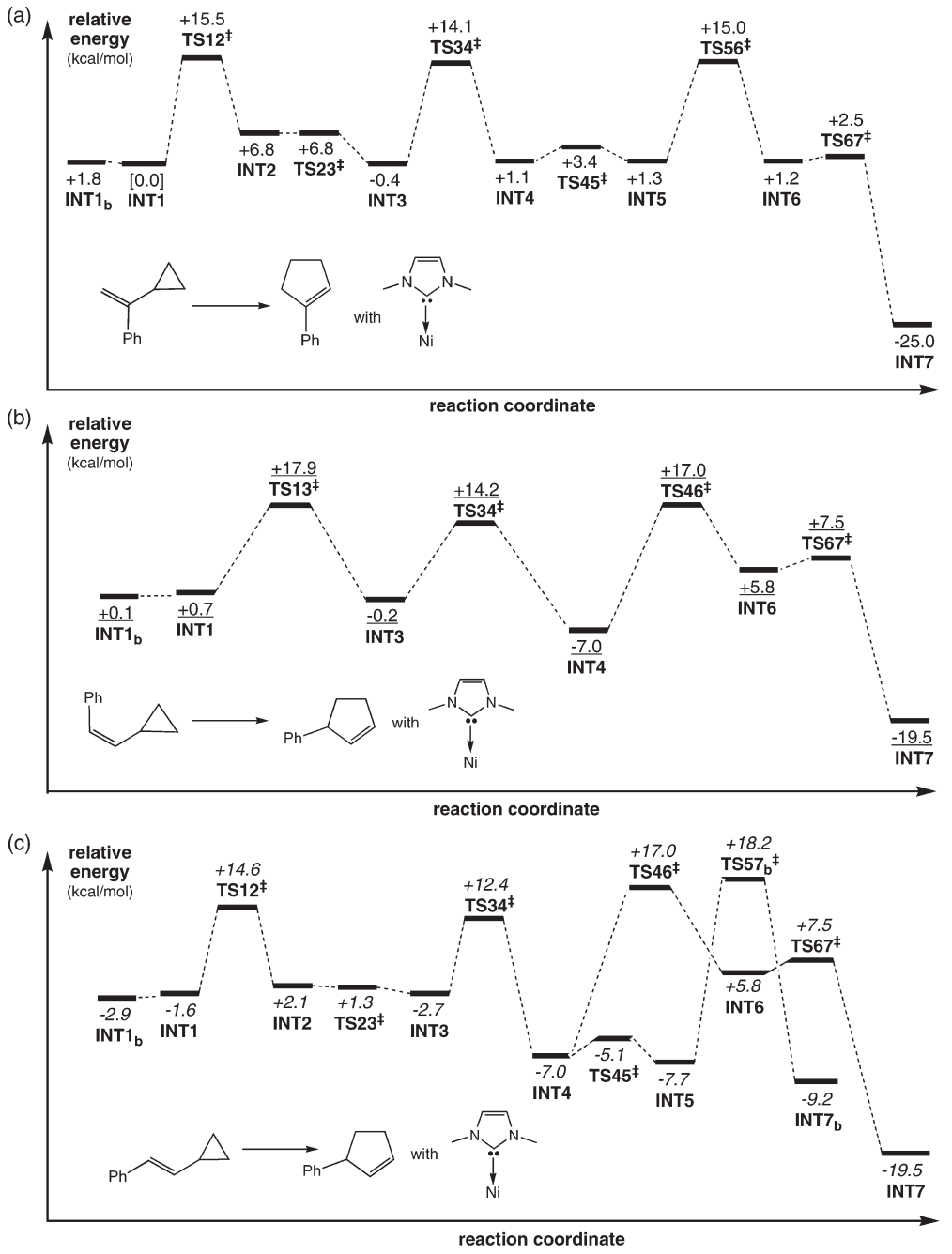

FIGURE 8. Relative energies (B3LYP/DZVP2+//B3LYP/LANL2DZ + ZPE(B3LYP/LANL2DZ), kcal/mol; see Computational Methods for details) of analogues of structures shown in Figure 1 with (a) internal phenyl-substituted vinylcyclopropane, (b) terminal *cis*-phenyl-substituted vinylcyclopropane, and (c) terminal *trans*-phenyl-substituted vinylcyclopropane.

(SIPr) is 3.2 times faster than the rearrangement of **2** in the presence of 1,3-bis(2,6-diisopropylphenyl)-imidazol-2-ylidene (IPr) (entries 1 and 2). Rearrangement is not observed with 1,3-bis(1,3,5-trimethylphenyl)-imidazol-2-ylidene (IMes) even under more forcing conditions (80 or 100 °C) and longer reaction times (16 h, entry 3). These results are consistent with previously reported vinylcyclopropane rearrangements in which use of the IMes ligand resulted in a dramatic decrease in yield.[8c] Rearrangement in the presence of $IPrCl_2$ is slightly faster than with the parent IPr ligand (entry 4, perhaps because $IPrCl_2$ is more robust than IPr). The difference in reactivity between the electronically similar IPr, SIPr, and IMes ligands suggests that steric factors play a significant role in the rearrangement, in that the NHCs with bulky isopropyl groups near the carbene center promoted reaction, whereas the one with only methyl groups near the carbene center (IMes) did not.

A variety of ligand/additive combinations were also examined in order to assess the composition of the active catalyst (Table 5). Interestingly, $Ni(IPr)_2$ without any additional additives promoted the rearrangement, although with a much lower yield and rate (entry 4, 32% yield and 14.2×10^{-3} s^{-1} first-order rate constant) than $Ni(COD)_2$ with IPr

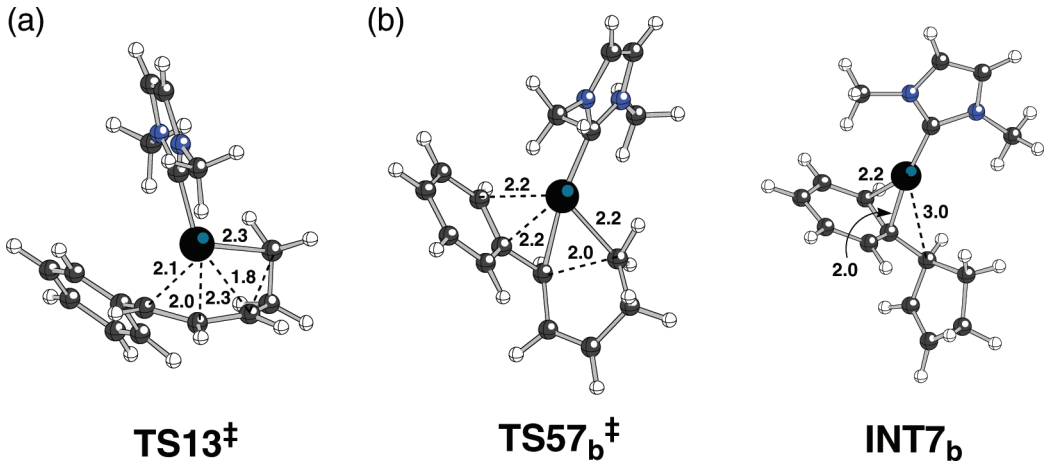

FIGURE 9. Computed geometries (B3LYP/LANL2DZ; distances in Å; see Computational Methods for details) of selected structures from (a) Figure 8b and (b) Figure 8c.

TABLE 2. Nickel-Catalyzed Isomerization of Various Vinyl Cyclopropanes

entry	Substrate	Product	T	rate (k)[a] $s^{-1}(10^{-3})$
1			27°C	25.1[b]
2			60°C	26.2[b]
3			27°C	19.8[b]
4			60°C	N.R.

[a]First-order rate constant (average of at least three runs). [b]Determined by NMR with ferrocene as an internal standard (average of at least three runs). N.R. = no reaction.

TABLE 3. Ni-Catalyzed Isomerization with Various Substrates[a]

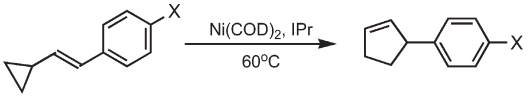

entry	X (compound no.)	rate $(k)^b$ s^{-1} $(10^{-3})^c$	yield $(\%)^d$	computed barrier (kcal/mol)[e,f]
1	CO_2Me (**5**)	98.6	93	18.1
2	CF_3 (**6**)	85.1	83	19.1
3	F (**7**)	32.7	82	19.3
4	H (**2**)	26.2	92	19.7
5	Me (**8**)	23.1	92	19.9
6	OMe (**9**)	11.7	72[g]	20.9

[a]Conditions: 5.0 mol % [$Ni(IPr)_2$], 10 mol % COD, and 0.20 M substrate in deuterated benzene. [b]First-order rate constant (average of at least three runs). [c]Determined by NMR with ferrocene as an internal standard (average of at least two runs). [d]Isolated yields, performed with 2.0 mol % [$Ni(COD)_2$], 4.0 mol % IPr, and 0.10 M substrate in hexanes. [e]Based on **INT1**; see Supporting Information for details. [f]The X = CN, NO_2 and NH_2 systems were also examined, and their computed barriers are 18.4, 18.5, and 20.8 kcal/mol, respectively; see Supporting Information for details. [g]GC yield.

additive (entry 1, 81% yield and 26.2×10^{-3} s^{-1} first-order rate constant). $Ni(IPr)_2$ with cyclooctadiene additive gave results (entry 2, 79% yield and 19.0×10^{-3} s^{-1} first-order rate constant) comparable to those of $Ni(COD)_2$ with IPr. When excess IPr was added to the $Ni(IPr)_2$ catalyst, the yield and rate (entry 3, 28% yield and 14.7×10^{-3} s^{-1} first-order rate constant) were comparable to those of $Ni(IPr)_2$ without an additive. Styrene and 1,5-dimethyl-cycloocta-1,5-diene were also examined as additives, and these led to slower reactions and lower yields than did $Ni(IPr)_2$ with COD additive. In addition, the optimized ratio of IPr to COD was determined to be 1:2. These results suggest that COD plays an important role in the formation (or stabilization) of the active catalyst.

In addition, calculations were performed on the rearrangement of the parent vinylcyclopropane system with other heterocyclic carbenes. Adding two chlorines to the imidazolylidene (Figure 11) seems to have only a very small effect on the rearrangement (the predicted overall barrier only changes from 16.8 to 16.5 kcal/mol), consistent with the experimental results in Table 4 (entries 2 and 4). Replacing one NR group of the imidazolylidene with an O or S is also predicted to have only small effects (Figure 11). These two ligands are sterically smaller than the corresponding imidazolylidenes, however, which could present a problem, as described above (also, vide infra). Overall, these results indicate that the rearrangement mechanism, from **INT1** to **INT7**, is not very sensitive to the electronic nature of the heterocyclic carbene ligand on Ni.

Rearrangement of the parent vinylcyclopropane system was also examined with trimethylphosphine as a simple model of alkyl phosphines (Figure 11). Although tricyclohexylphosphine was shown experimentally to be an ineffective ligand for promoting the rearrangement of unactivated vinylcyclopropanes,[8c] the computed mechanism and energetics for the trimethylphosphine-promoted rearrangement (Figure 11) are similar to those for the reaction with *N*,*N*′-dimethylimidazolylidene. Although the transition state structure for conversion of the η_1-alkyl/η_3-allyl intermediate to the metallacyclohexene intermediate becomes the rate-determining transition state structure in the phosphine

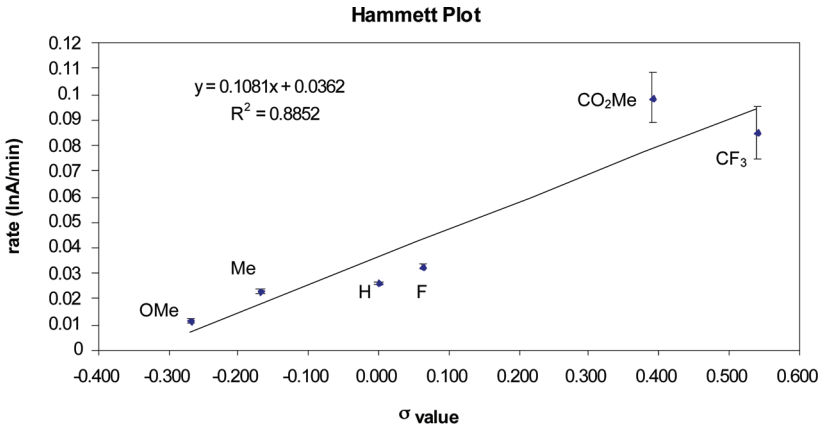

FIGURE 10. Hammett plot constructed from data in Table 3.[11]

TABLE 4. Ni-Catalyzed Isomerization with Various Ligands[a]

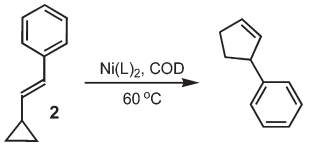

entry	Ligand	rate (k) $s^{-1}(10^{-3})$[a,b]	yield [%][c]
1	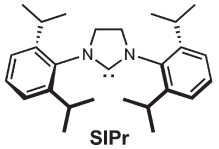 SIPr	85.0	87
2	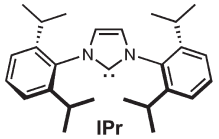 IPr	26.2	81
3	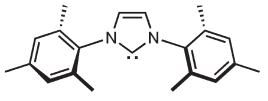 IMes	N.R.	
4	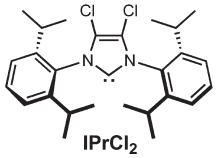 $IPrCl_2$	30.8	84

[a]Conditions: 5.0 mol % [$Ni(L)_2$], 10 mol % COD, and 0.20 M substrate in deuterated benzene. [b]First-order rate constant (average of at least three runs). [c]Determined by NMR with ferrocene as an internal standard (average of at least two runs). N.R. = No reaction.

system, the overall barrier predicted for rearrangement with trimethylphosphine is comparable to that predicted for rearrangement with *N*,*N*′-dimethylimidazolylidene. This suggests that the problem with phosphine ligands observed experimentally[8] may be related to initial formation of **INT1** rather than the subsequent rearrangement steps.

TABLE 5. Ni-Catalyzed Isomerization with Different Nickel Ligands (L) and Various Additives[a]

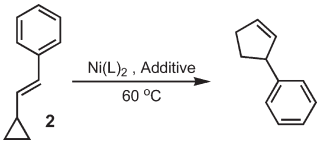

entry	Ligand (L)	Additive	rate (k) $s^{-1}(10^{-3})$[a,b]	yield[c]
1		**IPr**	26.2	81
2	**IPr**		19.0	79
3	**IPr**	**IPr**	14.7	28
4	**IPr**	----	14.2	32

[a]Conditions: 5.0 mol % [$Ni(L)_2$], 10.0 mol % additive, and 0.20 M substrate in deuterated benzene. [b]First-order rate constant (average of at least two runs). [c]Determined by NMR with ferrocene as an internal standard after three half-lives (average of at least two runs).

Taken together, this experimental and theoretical data hints that the most important difference between NHCs that promote rearrangement and NHCs and phosphines that do not may be their bulkiness. Our calculations indicate that in the absence of bulky groups, all of the ligand frameworks should allow for rearrangement. Our calculations also suggest, however, that two full-sized IPr ligands are unable to bind simultaneously to Ni when a vinylcyclopropane substrate is bound (i.e., optimization of such structures leads to dissociation of one IPr; see Supporting Information for details). Interestingly, a complex with two tricyclohexylphoshine ligands and a vinylcyclopropane substrate all bound to Ni could be located as a minimum. Thus, we suggest that the key role of bulky groups on IPr (and the related SIPr and $IPrCl_2$) is to promote dissociation of one NHC, allowing **INT1** to form; the smaller IMes and differently shaped phosphine ligands are less inclined to dissociate. The effectiveness of adding COD is also likely due to its ability to facilitate NHC dissociation.

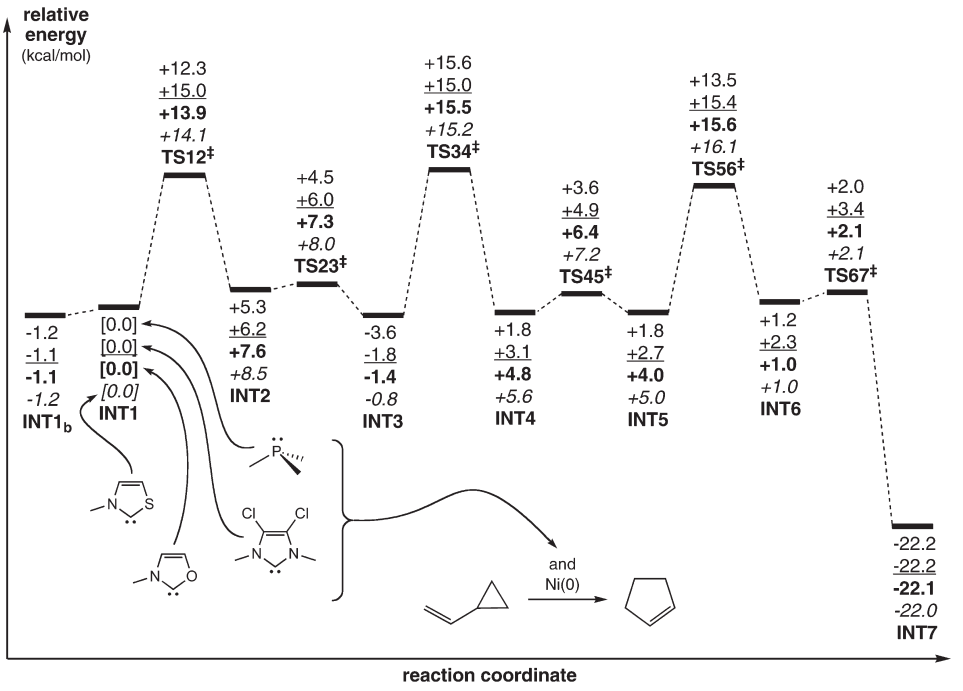

FIGURE 11. Relative energies (B3LYP/DZVP2+//B3LYP/LANL2DZ + ZPE(B3LYP/LANL2DZ), kcal/mol; see Computational Methods for details) of analogues of structures shown in Figure 1 with alternative ligands on Ni (trimethylphosphine in normal text, dichloro-*N*,*N*′-dimethylimidazolylidene in underlined text, *N*-methyloxazolylidene in **bold** text, *N*-methylthiazolylidene in *italic* text).[9]

Conclusion

We have proposed a catalytic cycle (Scheme 3) for the Ni(0)-catalyzed isomerization of vinylcyclopropanes to cyclopentenes based on physical organic experiments and theoretical calculations. Which step in this process is rate-determining appears to depend on the exact nature of the substrate used. In addition, the importance of generating a catalyst species with only one bound NHC was revealed, pointing to the importance of bulky groups on the NHC and the utility of COD as an additive. These results should aid the rational design of catalysts for additional substrates and asymmetric versions of this useful metal-promoted sigmatropic shift.

Experimental Section

Computational Methods. GAUSSIAN03[13] was used for all calculations. All geometries were optimized without symmetry constraints using B3LYP/LANL2DZ.[14] As a test, the B3LYP/LANL2DZ level was used to optimize the geometries of several Ni-allyl and Ni-NHC complexes for which X-ray structures have been reported, and no significant deviations between the computed and experimental geometries were observed (see Supporting Information for details). The vibrational frequencies of all stationary points were analyzed to characterize structures as minima or transition state structures. Intrinsic reaction coordinate (IRC) calculations[15] were used to further characterize the nature of some transition state structures by mapping out the portions of the reaction coordinates near to them (see Supporting Information for details). Geometries for the parent system (Figure 3) were also reoptimized using B3LYP/DZVP2+,[16] and no significant changes were observed (see Supporting Information for coordinates). Single point energies were calculated for all structures at the B3LYP/DZVP2+ level,[16] and these B3LYP/DZVP2+//B3LYP/LANL2DZ + ZPE(B3LYP/LANL2DZ) energies are reported throughout the text. (The corresponding energies from B3LYP/LANL2DZ + ZPE(B3LYP/LANL2DZ) calculations can be found in the Supporting Information). This theoretical approach has been used previously to characterize the chemistry of various organometallic complexes involving metals from the first transition series;[17] additional tests on the validity of this

(13) *GAUSSIAN03, revision B.04*; Frisch, M. J.; Trucks, G. W.; Schlegel, H. B.; Scuseria, G. E.; Robb, M. A.; Cheeseman, J. R.; Montgomery, J. A., Jr., Vreven, T.; Kudin, K. N.; Burant, J. C.; Millam, J. M.; Lyengar, S. S.; Tomasi, J.; Barone, V.; Mennucci, B.; Cossi, M.; Scalmani, G.; Rega, N.; Petresson, G. A.; Nakatsuji, H.; Hada, M.; Ehara, M.; Toyota, K.; Fukuda, R.; Hasegawa, J.; Ishida, M.; Nakajima, T.; Honda, Y.; Kitao, O.; Nakai, H.; Klene, M.; Li, X.; Knox, J. E.; Hratchian, H. P.; Cross, J. B.; Adamo, C.; Jaramillo, J.; Gomperts, R.; Stratmann, R. E.; Yazyev, O.; Austin, A. J.; R., Cammi; Pomelli, C.; Ochterski, J. W.; Ayala, P. Y.; Morokuma, K.; G. A, VothSalvador, P.; Dannenberg, J. J.; Zakrzewski, V. G.; Dapprich, S.; Daniels, A. D.; Strain, M. C.; Farkas, O.; Malick, D. K.; Rabuck, A. D.; Raghavachari, K.; Foresman, J. B.; Ortiz, J. V.; Cui, Q.; Baboul, A. G.; Clifford, S.; Cioslowski, J.; Stefanov, B. B.; Liu, G.; Liashenko, A.; Piskorz, P.; Komaromi, I.; Martin, R. L.; Martin, R. L.; Fox, D. J.; Keith, T.; Al-Laham, M. A.; Peng, C. Y.; Nanayakkara, A.; Challacombe, M.; Gill, P. M. W.; Johnson, B.; Chen, W.; Wong, M. W.; Gonzalez, C.; Pople, J. A. Gaussian, Inc.: Pittsburgh, PA, **2003**.

(14) (a) Becke, A. D. *J. Chem. Phys.* **1993**, *98*, 5648–5652. (b) Becke, A. D. *J. Chem. Phys.* **1993**, *98*, 1372–1377. (c) Lee, C.; Yang, W.; Parr, R. G. *Phys. Rev. B* **1988**, *37*, 785–789. (d) Stephens, P. J.; Devlin, F. J.; Chabalowski, C. F.; Frisch, M. J. *J. Phys. Chem.* **1994**, *98*, 11623–11627. (e) Hay, P. J.; Wadt, W. R. *J. Chem. Phys.* **1985**, *82*, 270–283.

(15) (a) Gonzalez, C.; Schlegel, H. B. *J. Phys. Chem.* **1990**, *94*, 5523–5527. (b) Fukui, K. *Acc. Chem. Res.* **1981**, *14*, 363–368.

(16) Braden, D. A.; Tyler, D. R. *J. Am. Chem. Soc.* **1998**, *120*, 942–947.

(17) (a) Tantillo, D. J.; Hoffmann, R. *Helv. Chim. Acta* **2001**, *84*, 1396–1404. (b) Tantillo, D. J.; Hoffmann, R. *J. Am. Chem. Soc.* **2001**, *123*, 9855–9859. (c) Tantillo, D. J.; Carpenter, B. K.; Hoffmann, R. *Organometallics* **2001**, *20*, 4562–4564. (d) Tantillo, D. J.; Hietbrink, B. N.; Merlic, C. A.; Houk, K. N. *J. Am. Chem. Soc.* **2000**, *122*, 7136–7137. (Additional note: *J. Am. Chem. Soc.* **2001**, *123*, 5851). (e) Merlic, C. A.; Walsh, J. C.; Tantillo, D. J.; Houk, K. N. *J. Am. Chem. Soc.* **1999**, *121*, 3596–3606. (f) Merlic, C. A.; Hietbrink, B. N.; Houk, K. N. *J. Org. Chem.* **2001**, *66*, 6738–6744. (g) Merlic, C. A.; Miller, M. M.; Hietbrink, B. N.; Houk, K. N. *J. Am. Chem. Soc.* **2001**, *123*, 4904–4918. (h) Hietbrink, B. N., Ph.D. Thesis, University of California, Los Angeles, **2000**.

theoretical approach for the Ni(0) systems explored herein are described below. In general, in order to reduce computational cost, the diisopropylphenyl groups of the IPr ligands were replaced by methyl groups (see Scheme 3). However, tests on the validity of this approximation were also performed using ONIOM(B3LYP/LANL2DZ:UFF) calculations[18] with full-sized carbene ligands. In these calculations, the quantum mechanics layer (treated with B3LYP/LANL2DZ) consisted of the vinylcyclopropane system, the Ni atom, and the heterocycle, while the molecular mechanics layer (treated with the Universal Force Field [UFF]) included the diisopropylphenyl groups. For the subset of structures from Figure 2 examined using this method, no significant changes to relative energies were observed (see Supporting Information for details), although we were not able to locate transition state structures for reductive elimination, where steric effects may be largest (vide infra). Structural drawings were produced using *Ball & Stick*.[19]

General Procedure for Rearrangement of Vinyl Cyclopropanes. In the drybox, vinyl cyclopropane was weighed directly into an oven-dried screw cap vial equipped with a magnetic stir bar and dissolved in hexane (0.1 M). A solution of $Ni(COD)_2$/IPr (2 mol %) ($Ni(COD)_2$ (1.0 equiv) and IPr (2.0 equiv) were dissolved in benzene and allowed to equilibrate at room temperature for 3 h) was added, and the vial was sealed with a PTFE-lined cap. The vial was removed from the drybox and the dark greenish-black reaction was stirred at 60 °C. After complete consumption of the substrate, the solvent was removed in vacuo, and the products were purified by silica gel chromatography. See Supporting Information for additional details.

General Procedure for Kinetic Experiments. A stock solution of vinyl cyclopropane and ferrocene (10 mol %) was prepared in deuterated benzene. A stock solution of $Ni(COD)_2$ (1.0 equiv) and IPr (2.0 equiv) was prepared in deuterated benzene and stirred for 4 h. The solution of vinyl cyclopropane (0.104 mmol) and ferrocene (0.0104 mmol) was syringed into an NMR with a screw cap. Deuterated benzene was added to give an overall solution of 0.2 M. The solution was then frozen in the glovebox before the $Ni(COD)_2$/IPr (0.00520 mmol) was added to prevent mixing. The NMR tube was frozen again after addition of the $Ni(COD)_2$/IPr solution and removed from the drybox. The NMR tube was warmed just before being placed in the NMR. The reaction was monitored by ^1H NMR, taking data points every minute. Reaction monitored for at least three half-lives. See Supporting Information for additional details.

Acknowledgment. We gratefully acknowledge the University of California−Davis, the National Science Foundation's CAREER and Partnership for Advanced Computational Infrastructure (PSC) programs, the American Chemical Society's Petroleum Research Fund (S.C.W. and D.J.T.), and the National Institutes of Health (all authors) for support.

Supporting Information Available: Coordinates and energies for all structures, IRC plots, additional computational data, and experimental details. This material is available free of charge via the Internet at http://pubs.acs.org.

(18) (a) Maseras, F.; Morokuma, K. *J. Comput. Chem.* **1995**, *16*, 1170–1179. (b) Vreven, T.; Morokuma, K.; Farkas, Ö.; Schlegel, H. B.; Frisch, M. J. *J. Comput. Chem.* **2003**, *24*, 760–769. (c) Svensson, M.; Humbel, S.; Morokuma, K. *J. Chem. Phys.* **1996**, *105*, 3654–3661.

(19) N. Müller Falk, A. *Ball & Stick V.3.7.6, molecular graphics application for MacOS computers*, Johannes Kepler University: Linz, **2000**.